ARTICLE IN PRESS

Ceramics International xxx (xxxx) xxx-xxx



Contents lists available at ScienceDirect

Ceramics International

journal homepage: www.elsevier.com/locate/ceramint



Effect of sintering temperature on phase constitution and mechanical properties of WC-1.0 wt% carbon nanotube composites

Tin Cao, Xiaoqiang Li*, Jingmao Li, Minai Zhang, Hao Qiu

National Engineering Research Center of Near-Net-Shape Forming for Metallic Materials, South China University of Technology, Guangzhou 510640, PR China

ARTICLE INFO

Keywords: Tungsten carbide Carbon nanotube Sintering temperature Transformation

ABSTRACT

Ultrafine grain WC-1.0 wt% carbon nanotube (CNT) composites were prepared using spark plasma sintering and the influence of sintering temperature on the properties of the composites was investigated. The specimen tested in this study achieved an optimum hardness of 22.81 ± 0.81 GPa and fracture toughness of 8.95 ± 0.38 MPa m^{1/2} after sintering at 1700 °C. On applying a sintering temperature of 1900 °C, the mechanical properties of the specimens deteriorated. Raman spectroscopic analysis results indicated that the structure of the CNTs changed and the graphite phase occurred at 1900 °C, which was responsible for the deteriorating hardness, elastic modulus, and fracture toughness. This study provides details of the transformation of the CNTs in the tungsten carbide matrix, indicating that the WC-CNT composites should be sintered at moderate temperatures.

1. Introduction

Owing to their unique mechanical properties, carbon nanotubes (CNTs) have been widely used for reinforcing various ceramic composites [1–12]. Binderless tungsten carbide (WC) ceramics exhibiting a strong resistance to wear and high-temperature corrosion are required to undergo a toughening process because of their shortcomings such as brittleness and low relative sintering density as compared to conventional WC-Co materials [13,14]. The toughening of micro-sized WC and WC-Co powder materials has been carried out by using CNTs as the toughening phase [15,16]. The presence of CNTs was found to be helpful for achieving densification wherein CNTs were a carbon source.

At the same time, WC might also affect the structure of the CNTs in the composites. Carbides usually require a high sintering temperature. In most instances, WC ceramics are sintered at a high temperature in order to ensure that they are fully compacted and the densification of pure WC and some WC-based composites generally ends at temperatures higher than 1800 °C [17–21]. As graphite cannot be observed by Raman spectroscopy when sintering temperature was not high enough, the conversion of CNTs to graphite can be identified from a shift in the G peak in their Raman spectra [15]. As it is unknown whether the structure of CNT is maintained at high sintering temperatures, it is worthwhile to investigate the effect of the sintering temperature on the WC-CNT composites.

In this study, an ultrafine grain, 1.0 wt% CNT-toughened WC composite (WC-1CNT) was used as the test material because it can be easily characterized, based on previously reported studies [1,7,16]. The

densification, microstructure, phase constitution, and mechanical properties of the *specimens* were investigated. Raman spectroscopic analysis revealed that the CNTs undergo phase transformation in the WC composite sintered at 1900 °C, which has not been observed to date in other CNT-toughened ceramics sintered at the same temperature.

2. Experimental

Commercially available WC powder (~0.2 μm, Golden Egret Special Alloy Co. Ltd., China) and multi-walled CNTs (MWCNTs) with an outer diameter of \sim 60–100 nm and length \sim 5–15 μm (Xuzhou Jiechuang New Material Technology Co. Ltd., China) were used as the starting materials. Appropriate amounts of the powders were mixed together to obtain a composition of WC and 1.0 wt% CNTs (WC-1CNT). The mixture was wet-milled on a planetary ball mill (QM-3SP2, Nanjing Nanda Instrument Plant, China) in ethanol for 30 h by using cemented carbide milling balls (ball-to-powder weight ratio of 4:1) and cemented carbide vials (250 mL). The milled powder was dried and sieved to remove any agglomerates which may lead to poor sinterability. The obtained WC-1CNT powder was poured into a cylindrical graphite die with an inner diameter of 20 mm and an outer diameter of 50 mm. The sintering was carried out on a Dr. Sinter Model SPS-825 spark plasma sintering (SPS) system (Sumitomo Coal Mining Co. Ltd., Japan) under vacuum (≤ 6 Pa). The specimens were sintered at temperatures ranging from 1600 to 1900 °C without soaking time. A heating rate of 100 °C min⁻¹ and an applied pressure of 10 MPa were used during processing. In the sintering process, graphite paper was used to separate the powder from the

E-mail address: lixq@scut.edu.cn (X. Li).

http://dx.doi.org/10.1016/j.ceramint.2017.09.154

Received 19 April 2017; Received in revised form 17 September 2017; Accepted 19 September 2017 0272-8842/ © 2017 Published by Elsevier Ltd.

^{*} Corresponding author.

T. Cao et al. Ceramics International xxxx (xxxxx) xxxx—xxx

graphite die or punches, and the die was surrounded with a porous carbon belt insulation in order to minimize radiation heat loss. An infrared pyrometer ($\geq 570\,^{\circ}\text{C}$) was focused at the bottom of the central core hole in the die wall, 7.5 mm away from the inner wall. The specimens sintered at different temperatures were named as WC-1CNT1600, WC-1CNT1700, WC-1CNT1800, and WC-1CNT1900.

The density of the sintered specimens was determined using water based on the Archimedes principle. The hardness (HV_{10}) was evaluated using a Vickers hardness tester (2100B, Wilson Wolpert Co. Ltd., China) with a load of 10 kgf. The reported values are the average of the data from five indentation tests. The Young's modulus of the composites was determined by a non-destructive test via the pulse-echo overlap ultrasonic technique. The fracture toughness (K_{IC}) was calculated according to the Anstis equation, based on a radial crack produced by the Vickers (HV_{10}) indentation [22].

After polishing, the phase constitution was analyzed by using an X-ray diffractometer (XRD, D8 Advance, Bruker Co., Germany) and a Raman spectrometer (LabRam Aramis, H.J.Y Co. Ltd., France). The indentation traces and crack details of the specimens were examined by high-resolution scanning electron microscopy (HRSEM, Nova Nano 430, FEI, USA) after corrosion. The fracture surfaces were directly examined by HRSEM.

3. Results and discussion

3.1. Densification behavior

Fig. 1 shows the densification curve of the WC-1CNT1900 specimen. Before starting the real densification of the powder, the punch displacement was increased in a direction opposite to the shrinkage direction owing to the thermal expansion of the compacted powder specimen and/or the punches. As the shrinkage rate turned positive, densification of the powder started to take place and persisted until the shrinkage rate decreased to zero. The sintering behavior of WC-1CNT is similar to that of over-stoichiometric binderless WC materials in which the presence of excess carbon facilitated a decrease in the final densification temperature [20,21]. For all the specimens, the densification process started at ~950 °C and ended at ~1650 °C. On further increasing the temperature, the shrinkage rate again fluctuated around zero. The densities of the sintered specimens are listed in Table 1. At temperatures < 1700 °C, the sintered specimen could not be densified. Relative densities higher than 100% were achieved because of the consumption of CNTs.

3.2. Phase constitution and microstructure

Fig. 2 shows the XRD patterns of WC-1CNT specimens sintered at different temperatures. The crystal structure of the sintered specimens corresponds to the hexagonal WC structure. The diffraction peaks of CNT are inconspicuous because of its low fraction in the specimen. For

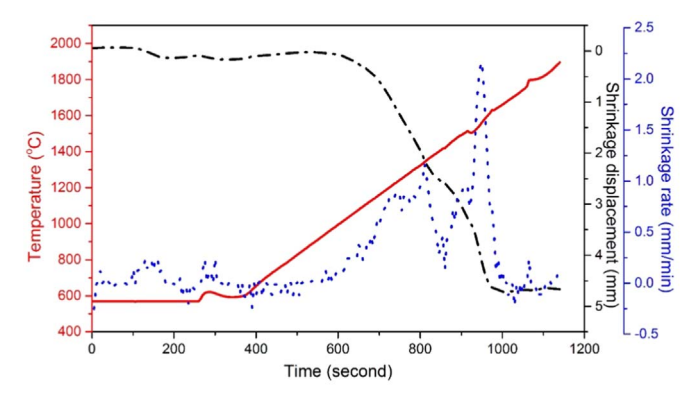


Fig. 1. Densification curves of WC-1CNT1900.

Table 1
Characteristics of the WC-1CNT specimens sintered at different temperatures.

Sintering temperature (°C)	Density (g cm ⁻³)	Relative density (%)	Hardness (GPa)	Young's Modulus (GPa)	Fracture toughness (MPa m ^{1/2})
1600	13.48	93	18.35 ± 0.75 22.81 ± 0.81 22.25 ± 0.53 20.73 ± 0.13	506	9.11 ± 0.55
1700	14.86	101		658	8.95 ± 0.38
1800	14.93	102		632	8.92 ± 0.46
1900	14.82	100		531	6.87 ± 1.73

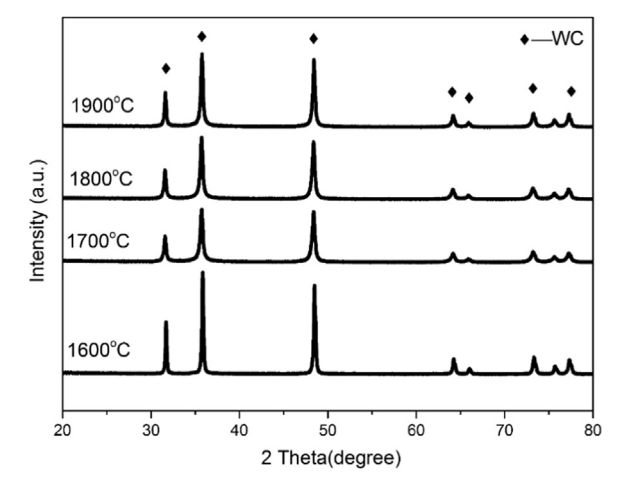


Fig. 2. XRD patterns of the specimens sintered at different temperatures.

all the sintered specimens, no peaks other than those corresponding to WC were observed. Thus, the formation of a carbon-deficient W_2C was effectively inhibited by sintering and by the addition of CNTs. As shown in Fig. 3, pores are still present in the WC-1CNT1600 specimen, while the WC-1CNT1700 and WC-1CNT1800 specimens exhibit clear grain boundaries. However, "blurry" grain boundaries are observed in the WC-1CNT1900 specimen, partly because of the high carbon content. This phenomenon can be explained by Raman spectroscopy, which is a conventional method for identifying different carbon structures.

Fig. 4 shows the Raman spectra of pure CNT, the milled WC-CNT powder, and the sintered WC-1CNT specimens. The position and intensity ratios of the observed peaks were examined in order to understand the chemical and structural changes of the CNTs [23]. All peaks shifted toward a higher energy after sintering as a result of a decrease in the average distance between the defects and the residual compressive stress induced on the CNT network formed by the ceramic matrix during the cooling step [1]. The ratio of the intensities of the D and G bands (I_D/I_G) remained almost stable, indicating that no significant chemical damage occurred during the sintering process. In addition, the position of the G' band, which provides information about sp^2 carbon [23], shifted toward higher wavenumbers with an increase in temperature, as displayed in Fig. 4. The G' band disappeared on increasing the final temperature to 1900 °C, implying that the structural consistency of sp^2 carbon was affected by the strong interactions between the CNTs and WC during sintering at 1900 °C, and unclear grain boundaries were observed due to the high carbon content.

CNTs can be transformed into other phases in SPS processing. F.M. Zhang et al. have reported the conversion of CNTs into diamonds during SPS (> 1200 °C) of MWCNTs [24]. Besides the diamond phase, Shi et al. have inferred the formation of graphite on MWCNTs coated with WC in the WC-Co composite from a shift in the G band in the Raman spectra [15]. WC-Co materials are sintered at low temperatures, which makes it difficult to observe the existence of graphite owing to its small quantity. As shown in Fig. 5, the diamond and the graphite phases could be detected in WC-1CNT1600 and WC-1CNT1900, respectively. In contrast, the CNT structure remained intact on sintering CNT in ZrB₂ at

Download English Version:

https://daneshyari.com/en/article/7888824

Download Persian Version:

https://daneshyari.com/article/7888824

<u>Daneshyari.com</u>